Atmos. Meas. Tech. Discuss., doi:10.5194/amt-2016-83, 2016
Manuscript under review for journal Atmos. Meas. Tech.
Published: 15 March 2016

Atmospheric Measurement Techniques Discussions

Errors in radial velocity variance from Doppler wind lidar

Hui Wang[1], Rebecca J. Barthelmie[1], Paula Doubrawa[1], and Sara C. Pryor[2]

[1]Sibley School of Mechanical and Aerospace Engineering, Cornell University, Ithaca, NY 14853
[2]Department of Earth and Atmospheric Sciences, Cornell University, Ithaca, NY 14853

Correspondence to: Hui Wang (hw524@cornell.edu)

Abstract. A high-fidelity lidar turbulence measurement technique relies on accurate estimates of radial velocity variance that are subject to both systematic and random errors determined by the autocorrelation function of radial velocity, the sampling rate, and the sampling duration. Using both statistically simulated and observed data, this paper quantifies the effect of the volumetric averaging in lidar radial velocity measurements on the autocorrelation function and the dependence of the systematic and random errors on the sampling duration. For current generation scanning lidars and sampling durations of about 30 minutes and longer during which the stationarity assumption is valid for atmospheric flows the systematic error is negligible but the random error exceeds about 10 %.

1 Motivation and approach

Coherent Doppler lidars (hereafter called lidars) are increasingly being deployed to measure flow in the atmospheric boundary layer (ABL) particularly for applications to wind engineering (e.g. Banta et al. (2013)). Accordingly, uncertainties in lidar-derived mean wind velocity estimates have been well characterized (Wang et al., 2015; Lindelöw-Marsden, 2009) and methods and procedures have been developed for error reduction and uncertainty control (Gottschall et al., 2012; Clifton et al., 2013). However, use of lidar for turbulence measurements, while possible (Mann et al., 2010; Branlard et al., 2013; Newman et al., 2015), is less established (Sathe and Mann, 2013; Sathe et al., 2015)

Virtually all approaches for deriving the second order moments of the flow are predicated on the radial velocity variance (Sathe and Mann, 2013; Newman et al., 2015). Thus, improved understanding of errors in lidar-derived radial velocity variance estimates is a necessary pre-requisite to the development of robust techniques that will enable the widespread use of lidar for high-fidelity turbulence measurements. Accordingly, the objectives of this work are to improve the characterization of radial velocity variance error properties and to develop tools to quantify and reduce these errors. The approach taken and the format of this paper are as follows: the theoretical framework used herein to quantify errors in radial velocity variance from lidar measurements leverages that developed to characterize uncertainties in statistical moments estimated from time series of sonic anemometer measurements in Lenschow et al. (1994), and is modified to incorporate the effect of volumetric averaging and the slow sampling rate (Sect. 3). The theoretical findings are then validated using empirical estimates obtained from measurements of a Galion lidar and three co-deployed sonic anemometers (Sect. 4). The theoretical framework is then used to investigate the sampling duration required to obtain a pre-defined error magnitude (Sect. 5).

Atmos. Meas. Tech. Discuss., doi:10.5194/amt-2016-83, 2016
Manuscript under review for journal Atmos. Meas. Tech.
Published: 15 March 2016

Atmospheric Measurement Techniques Discussions

2 Preliminaries

A brief description of lidar measurements is given below. For more details see Mann et al. (2008) and Sathe and Mann (2012).

Denoting a wind velocity vector as:

$$\boldsymbol{u} = (u_1, u_2, u_3) \tag{1}$$

where u_1, u_2 and u_3 are streamwise, transverse and vertical wind components respectively at position $\boldsymbol{x} = (x_1, x_2, x_3)$. Without loss of generality, we can assume that the mean streamwise velocity U_1 has been removed and $\boldsymbol{u}$ only consists of the fluctuating components of turbulence with zero means. A lidar measures the radial velocity (v_r) from the Doppler frequency shift induced by the motion of scatterers along the line of sight (LOS), where the orientation of LOS is defined by the unit directional vector:

$$\boldsymbol{n} = (\cos\phi\sin\theta, \cos\phi\cos\theta, \sin\phi) \tag{2}$$

where θ is the azimuth angle that increases clockwise from being zero in positive x_2 direction and ϕ is the elevation angle relative to the x_1–x_2 plane. The radial velocity is the projection of wind velocity on the LOS and is defined as:

$$v_\mathrm{r} = \boldsymbol{n} \cdot \boldsymbol{u} \tag{3}$$

For a pulsed lidar, each radial velocity is measured over a dwell time of approximately $1.0\,\mathrm{sec}$ during which spectra of a large number of returned signals are averaged to improve the measurement accuracy. When operated with a scan geometry, the lidar steers its transceiver to probe at different sets of θ and ϕ. Hence, the sampling interval of two consecutive measurements at one location depends on the dwell time, the scan geometry, and the mechanical design of the lidar. The shortest sampling interval can be achieved with the staring scan for which the lidar measures with fixed θ and ϕ, that is, the sampling interval is close to the dwell time. Each measured radial velocity (v_R) is estimated from an averaged spectrum acquired over a range gate; hence, it is a weighted average of radial velocities along the LOS:

$$v_\mathrm{R}(s) = \int_{-\infty}^{+\infty} Q(s') v_\mathrm{r}(s - s')\mathrm{d}s' \tag{4}$$

where s denotes the range gate location and s' is the range distance on the LOS. Note that we use R as the subscript to denote an average quantity and r to denote a point quantity. The weighting function Q in Eq. (4) can be approximated by the Gaussian function (Kristensen et al., 2011):

$$Q(s') = \frac{1}{\sqrt{2\pi}\sigma_\mathrm{Q}} \exp\left[-\frac{(s'-s)^2}{2\sigma_\mathrm{Q}^2}\right] \tag{5}$$

where the standard deviation σ_Q is a measure of the volumetric averaging size, and it is $15.4\,\mathrm{m}$ for the Galion lidar used herein (Wang et al., 2015).

The covariance of v_r (R_r) and v_R (R_R) along the x_1 direction are defined as follows (Mann et al., 2008):

$$R_\mathrm{r}(r_1) = n_i n_j R_{ij}(r_1 \boldsymbol{e}_1) \tag{6}$$

Atmos. Meas. Tech. Discuss., doi:10.5194/amt-2016-83, 2016
Manuscript under review for journal Atmos. Meas. Tech.
Published: 15 March 2016

Atmospheric Measurement Techniques Discussions

$$R_{\mathrm{R}}(r_1) = n_i n_j \int_{-\infty}^{+\infty}\int Q(s')Q(s'')R_{ij}\Big((s''-s')\boldsymbol{n} + r_1\boldsymbol{e}_1\Big)\mathrm{d}s'\mathrm{d}s'' \tag{7}$$

where s' and s'' denote the range distance, R_{ij} is the velocity tensor for the ith and jth velocity components, n_i and n_j are the components of $\boldsymbol{n}$, and $\boldsymbol{e}_1$ and r_1 are the unit vector and the separation distance on the x_1 axis, respectivley. Note that $i, j = 1, 2, 3$ and summation is assumed over repeated indices. We can map r_1 to the temporal lag τ through the frozen turbulence hypothesis (Taylor, 1938); $r_1 = U_1\tau$. The spatial autocorrelation function of v_{r} (ρ_{r}) and v_{R} (ρ_{R}) separated by $(r_1, 0, 0)$ are then defined respectively as:

$$\rho_{\mathrm{r}}(r_1) = R_{\mathrm{r}}(r_1)/\mu_{2,\mathrm{r}} \tag{8}$$

$$\rho_{\mathrm{R}}(r_1) = R_{\mathrm{R}}(r_1)/\mu_{2,\mathrm{R}} \tag{9}$$

where $\mu_{2,\mathrm{r}} = R_{\mathrm{r}}(0)$ is the variance of v_{r} and $\mu_{2,\mathrm{R}} = R_{\mathrm{R}}(0)$ is the variance of v_{R}. Due to the averaging given in Eq. (4), $R_{\mathrm{R}}(0) < R_{\mathrm{r}}(0)$ and the ratio $R_{\mathrm{R}}(0)/R_{\mathrm{r}}(0)$ decreases when the size of volumetric averaging increases (i.e., σ_{Q}/L_1 increases where L_1 is the integral length scale of u_1) (Mann et al., 2008). However, $R_{\mathrm{R}}(r_1) = R_{\mathrm{r}}(r_1)$ when r_1 is sufficiently large (e.g., $r_1 \gg L_1$), because values of $R_{\mathrm{r}}(r_1)$ with large r_1 are determined by eddies of large sizes that are not affected by the averaging. As illustrated in Fig. 1, assuming that turbulence is isotropic, $R_{\mathrm{R}}(r_1)$ starts at a value lower than $R_{\mathrm{r}}(r_1)$ at $r_1 = 0$ and gradually converges to $R_{\mathrm{r}}(r_1)$ as r_1 increases. Because $R_{\mathrm{r}}(0)$ and $R_{\mathrm{R}}(0)$ are the denominators in Eqs. (8) and (9), respectively, $\rho_{\mathrm{R}} \geq \rho_{\mathrm{r}}$ and $(\rho_{\mathrm{R}} - \rho_{\mathrm{r}})$ increases with increasing σ_{Q}/L_1. As a result, if we denote L_{r} and L_{R} respectively as the integral lenght scales for v_{r} and v_{R}, $L_{\mathrm{R}} > L_{\mathrm{r}}$ and $L_{\mathrm{R}}/L_{\mathrm{r}}$ increases with increasing σ_{Q}/L_1 (Fig. 1). Although quantitative evaluation of $R_{\mathrm{R}}/R_{\mathrm{r}}$ or $(\rho_{\mathrm{R}} - \rho_{\mathrm{r}})$ as a function of r_1 requires knowledge of velocity tensors R_{ij}, the qualitative statement above is also true for non-isotropic turbulence and has implications on the errors of radial velocity variance estimates as demonstrated in the next section.

3 Errors in radial velocity variance

In the following, the analysis and notation used are from Lenschow et al. (1994), and we use the word error to refer to the error of radial velocity variance estimated from time series.

Radial velocity variance is estimated from time series of radial velocity that is related to $\boldsymbol{u}(t)$ which is a stationary and ergodic time series generated from a Gaussian process characterized by the mean wind speed U_1 and covariance tensors. Assuming that the mean has been removed from $\boldsymbol{u}(t)$, it can be shown that both v_{r} and v_{R} are also from a stationary and ergodic time series of a Gaussian process that has the following properties:

- Zero ensemble mean for both v_{r} and v_{R}
- Ensemble variance $\mu_{2,\mathrm{r}} = \langle v_{\mathrm{r}}^2 \rangle$ and $\mu_{2,\mathrm{R}} = \langle v_{\mathrm{R}}^2 \rangle$

Atmos. Meas. Tech. Discuss., doi:10.5194/amt-2016-83, 2016
Manuscript under review for journal Atmos. Meas. Tech.
Published: 15 March 2016

Atmospheric Measurement Techniques Discussions

– Ensemble autocorrelation $\rho_{\mathrm{r}}(\tau)$ and $\rho_{\mathrm{R}}(\tau)$

The systematic and random errors are derived in the following for a disjunct time series of v_{r}, but the results can be used for v_{R}. As discussed in more detail in the subsequent text, the difference between v_{r} and v_{R} in terms of the relative errors derives solely from the difference between ρ_{r} and ρ_{R}.

Radial velocity measurements from a pulsed lidar naturally form a discrete time series (see Sect. 2). If a pulsed lidar is operated with the VAD technique to estimate turbulence statistics (e.g., Sathe et al. (2015)), the lidar samples at least six locations sequentially and therefore the sampling interval (δt) at one location is at least six times the sampling interval per one lidar measurement (i.e., $\delta t > 6\,\mathrm{sec}$ and is at least 60 times slower than a sonic anemometer sampling at 10 Hz). Hence, the radial velocity variance from a time series of v_{r} acquired over a period T with a sampling interval δt is estimated from:

$$\mu_{2,\mathrm{r}}(T) = \frac{1}{N}\sum_{i=1}^{N}\left[v_{\mathrm{r}}(t_i) - \mu_{1,\mathrm{r}}(T)\right]^2 \tag{10}$$

where t_i is the time stamp of measurement, $N = 1 + T/\delta t$ is the sample number, and $\mu_{1,\mathrm{r}}(T)$ is the ensemble mean estimate:

$$\mu_{1,\mathrm{r}}(T) = \frac{1}{N}\sum_{i=1}^{N} v_{\mathrm{r}}(t_i) \tag{11}$$

The radial velocity variance estimated from Eq. (10) has a systematic error $E_{\mathrm{s,r}}$ given by:

$$E_{\mathrm{s,r}} = \langle\mu_{2,\mathrm{r}}(T)\rangle - \mu_{2,\mathrm{r}} = -\langle\mu_{1,\mathrm{r}}^2(T)\rangle \tag{12}$$

Note that $\langle\mu_{1,\mathrm{r}}^2(T)\rangle$ is the sample mean variance; hence the systematic error is always negative, and its relative magnitude is given by Box et al. (2015):

$$e_{\mathrm{s,r}} = -\frac{E_{\mathrm{s,r}}}{\mu_{2,\mathrm{r}}} = \frac{S_{1,\mathrm{r}}}{N^2} \tag{13}$$

where

$$S_{1,\mathrm{r}} = \sum_{i=1}^{N}\sum_{j=1}^{N}\rho_{\mathrm{r}}(t_i - t_j) \tag{14}$$

Each radial velocity variance estimated from Eq. (10) also has a random error relative to the expected value of the estimate $\langle\mu_{2,\mathrm{r}}(T)\rangle$ that has zero mean and variance defined as:

$$E_{\mathrm{r,r}}^2 = \left\langle\left[\mu_{2,\mathrm{r}}(T) - \langle\mu_{2,\mathrm{r}}(T)\rangle\right]^2\right\rangle \tag{15}$$

Applying the Isserlis relation of a Gaussian process (Lenschow et al., 1994), it can be shown that the relative random error variance is:

$$e_{\mathrm{r,r}}^2 = \frac{E_{\mathrm{r,r}}^2}{\mu_{2,\mathrm{r}}^2} = \frac{2}{N^4}S_{1,\mathrm{r}}^2 + \frac{2}{N^2}S_{2,\mathrm{r}} - \frac{4}{N}S_{3,\mathrm{r}} \tag{16}$$

Atmos. Meas. Tech. Discuss., doi:10.5194/amt-2016-83, 2016
Manuscript under review for journal Atmos. Meas. Tech.
Published: 15 March 2016

Atmospheric Measurement Techniques Discussions

where

$$S_{2,\mathrm{r}} = \sum_{i=1}^{N}\sum_{j=1}^{N}\left[\rho_{\mathrm{r}}(t_i - t_j)\right]^2 \tag{17}$$

$$S_{3,\mathrm{r}} = \sum_{i=1}^{N}\sum_{m=1}^{N}\sum_{n=1}^{N}\left[\rho_{\mathrm{r}}(t_i - t_m)\right]\left[\rho_{\mathrm{r}}(t_n - t_i)\right] \tag{18}$$

The error expressions derived in Eqs. 13 and 16 are valid for v_{R} variance with the replacement of the autocorrelation and the variance by ρ_{R} and $\mu_{2,\mathrm{R}}$, respectively.

It is clear from Eqs. (13) and (16) that the errors are functions of the sampling interval, the sampling duration and the autocorrelation function. The averaging defined in Eq. (4) affects the shapes of the radial velocity covariance and autocorrelation function as illustrated using the isotropic turbulence model (Fig. 1). To investigate the impact of anisotropic turbulence under realistic atmospheric conditions, wind vectors are statistically simulated from the Risø Smooth Terrain (SMOOTH) spectrum model using TurbSim (2016). The simulation domain is $725 \times 60 \times 12\,\mathrm{m}$ ($x_1 \times x_2 \times x_3$) centered at 80 m above the ground, and has a horizontal and vertical resolution of 1.0 and 0.5 m, respectively. In these simulations the mean wind speed is $8\,\mathrm{ms}^{-1}$ and the time interval is 0.125 sec. Point radial velocities (v_{r}) are calculated using Eq. (3) for varying LOS orientations in the horizontal plane relative to the x_1 direction (denoted by β) with a fixed elevation angle of 10°. Lidar-equivalent radial velocities (v_{R}) are derived by averaging v_{r} on the LOS within $\pm 30\,\mathrm{m}$ from the domain center using the weighting function in Eq. (5). As expected, variance reduction occurs for all LOS orientations. The difference between R_{R} and R_{r} in Fig. 2 is similar to that in Fig. 1, and can be explained using the structure function (D_{r}) defined as:

$$D_{\mathrm{r}}(\tau) = 2\left[R_{\mathrm{r}}(0) - R_{\mathrm{r}}(\tau)\right] \tag{19}$$

for a given time lag (τ) and used to represent the energy of eddies of sizes that are smaller than the scale $U_1\tau$ (Pope, 2000). Volumetric averaging only attenuates the energy of eddies of small size (Mann et al., 2008). When τ is small relative to the integral time scale τ_0, volumetric averaging causes $D_{\mathrm{r}}(\tau)$ to decrease; hence, R_{R} decreases slower than R_{r} with respect to τ per Eq. (19). When τ/τ_0 is large (e.g., $\tau/\tau_0 > 0.25$), $R_{\mathrm{R}} = R_{\mathrm{r}}$, because volumetric averaging has little effect on eddies of scales of large τ. The difference between R_{R} and R_{r} results in $\rho_{\mathrm{R}} > \rho_{\mathrm{r}}$ for all time lags and LOS orientations (Fig. 2). Simulations conducted with the Kaimal (IECKAI) spectrum model TurbSim (2016) produce similar results. Errors associated with the autocorrelation functions $\rho_{\mathrm{r}}/\rho_{\mathrm{R}}$ derived from the simulated $v_{\mathrm{r}}/v_{\mathrm{R}}$ from both models are shown in Fig. 3. Although the difference between the errors of variance of v_{r} and v_{R} varies with LOS orientation and turbulence model (i.e. the turbulence structure), errors associated with v_{R} are consistently higher than those related to v_{r}, indicating volumetric averaging increases errors associated with radial velocity variance estimates.

Thus both the statistically simulated wind data and physical reasoning provide evidence that volumetric averaging increases the autocorrelation of radial velocity and inflate the errors in radial velocity variance estimates. Further confirmation will be provided in the next section, where data from a field experiment are used to show the effects of volumetric averaging and sampling duration on the errors.

Atmos. Meas. Tech. Discuss., doi:10.5194/amt-2016-83, 2016
Manuscript under review for journal Atmos. Meas. Tech.
Published: 15 March 2016

Atmospheric Measurement Techniques Discussions

4 Errors from observations

4.1 Experiment setup

Measurements presented herein were obtained during the Prince Edward Island Wind Energy Experiment (PEIWEE) conducted at the Wind Energy Institute of Canada (WEICan) site on the North Cape of PEI (Barthelmie et al., 2016). During the experiment a Galion lidar was configured with 20 kHz pulse repletion frequency and 1.0 sec dwell time to scan at four elevation angles (4.8°, 10.0°, 15.2° and 20.6°) wiht a fixed azimuth angle of 349° such that the 7th range gate of the lidar sampled at 20 m, 40 m, 60 m (and 80 m) above the ground where three Gill Windmaster Pro sonic anemometers were installed on a slender meteorological mast and sampled at 10 Hz. The sampling interval of the lidar at each elevation angle is about 7.5 sec, which is similar to the sampling interval of the 6–beam technique used for turbulence measurement in Sathe et al. (2015).The measurements from the sonic anemometers are used to describe the atmospheric turbulence conditions and evaluate the accuracy of the lidar measurements.

The lidar conducted automatic cleaning at the beginning of each hour, resulting in a 60 sec gap in the measurements; thus analysis presented here uses a sample period of one hour. Comparison of the hourly mean and variance of radial velocities from the lidar and sonic anemometers indicates good agreement (the correlation coefficient = 0.998) with the exception of periods when the measurements were in the wake of a wind turbine located 60 m southwest of the Galion (Fig. 4). The variance is consistently higher (on average by 19%) for the sonic radial velocity than the lidar radial velocity because of the expected attenuation in variance caused by volumetric averaging.

Stationarity is the fundamental assumption required to obtain theoretical estimates of the errors (as in Sect. 3). Thus, the lidar radial velocity data are evaluated for stationarity using the approach of Foken and Wichura (1996). Each hourly time series is evenly divided into 12 subsets. If the mean of the variance of the subsets deviates by less than 30% from the variance of the hourly time series, the time series is considered to be stationary. Among all the hourly time series obtained at the three heights, 33 pass the stationarity test and have concurrent sonic data (Fig. 4); therefore, they are used to derive the empirical estimates of errors.

4.2 Error estimation method

The systematic error $e_{\mathrm{s}}(T_{\mathrm{n}}, T)$ and random error variance $e_{\mathrm{r}}^2(T_{\mathrm{n}}, T)$ associated with the sampling duration T_{n} derived from a time series of length T are estimated using the stationary bootstrap method (Politis and Romano, 1994) as follows where the sample numbers associated with T and T_{n} are denoted as N_{T} and N_{n}, respectively:

- A new time series of size of N_{T} is constructed by resampling blocks of the original time series. To keep the new time series stationary, the sizes of the blocks are randomly drawn from a geometric distribution and the locations (the start of each block) are randomly drawn from a discrete uniform distribution on $(1, 2, \ldots, N_{\mathrm{T}})$. The only parameter to be specified is the optimal mean block size for the geometric distribution which is found by minimizing the mean squared error of the estimate of the sample mean variance (Politis and White, 2004).

Atmos. Meas. Tech. Discuss., doi:10.5194/amt-2016-83, 2016
Manuscript under review for journal Atmos. Meas. Tech.
Published: 15 March 2016

Atmospheric Measurement Techniques Discussions

– A subset of size of $N_{\rm n}$ is randomly selected from the new time series and its mean and variance, denoted as $\mu_1(T_{{\rm n},i})$ and $\mu_2(T_{{\rm n},i})$, respectively, are recorded. The subscript i denotes that it is the ith resampling.

– Sequences of $\mu_1(T_{{\rm n},i})$ and $\mu_2(T_{{\rm n},i})$ are acquired after repeating the two steps above for $N_{\rm b}$ times. The variance of the sample mean $\langle\mu_1^2(T_{\rm n},T)\rangle$is approximated as:

$$\langle\mu_1^2(T_{\rm n},T)\rangle = \frac{1}{N_{\rm b}}\sum_{i=1}^{N_{\rm b}}\mu_1^2(T_{{\rm n},i}) \tag{20}$$

– Per the definition in Eq. (12), the systematic error $e_{\rm s}(T_{\rm n},T)$ can be calculated as:

$$e_{\rm s}(T_{\rm n},T) = \frac{\langle\mu_1^2(T_{\rm n},T)\rangle}{\mu_2(T)} \tag{21}$$

– To calculate the random error variance, the expected value $\langle\mu_2(T_{\rm n},T)\rangle$ is first estimated by adding the systematic error to μ_2 which is approximated by $\mu_2(T)$, i.e.,

$$\langle\mu_2(T_{\rm n},T)\rangle = \mu_2(T) - \langle\mu_1^2(T_{\rm n},T)\rangle \tag{22}$$

Then the random error variance is derived with the following equation:

$$e_{\rm r}^2(T_{\rm n},T) = \frac{\frac{1}{N_{\rm b}}\sum_{i=1}^{N_{\rm b}}\left[\mu_2(T_{{\rm n},i}) - \langle\mu_2(T_{\rm n},T)\rangle\right]^2}{\mu_2^2(T)} \tag{23}$$

4.3 Observed errors

Two methods are used to estimate the errors associated with different sampling durations after the means are removed from the hourly time series of the point radial velocity from sonic anemometers ($v_{\rm r,sonic}$) and the lidar-measured averaged radial velocity ($v_{\rm R,lidar}$). The first method, denoted as the M_ρ method, is based on Eqs. (13) and (16) and the autocorrelation function derived from measurements (Fig. 5a). The observed autocorrelation functions show the postulated effect of volumetric averaging on the autocorrelation function. For all the hourly time series studied here, the autocorrelation of $v_{\rm R,lidar}$ at time lag one (τ = 7.5 sec) is significantly higher than that of $v_{\rm r,sonic}$ (Fig. 6). At time lag two (τ = 15 sec), the autocorrelation of $v_{\rm R,lidar}$ is still larger than that of $v_{\rm r,sonic}$, but the difference is not always statistically significant. Beyond time lag two (τ > 15 sec), the difference between the autocorrelation of $v_{\rm R,lidar}$ and $v_{\rm r,sonic}$ vanishes. Because integral time scales of streamwise velocity calculated from the sonic data are all below 30 sec, we assume that the autocorrelation function values of both $v_{\rm r,sonic}$ and $v_{\rm R,lidar}$ are zero for time lags larger than 60 sec. The autocorrelation-based systematic error and random error variance will be denoted as $e_{{\rm s},\rho}$ and $e_{{\rm r},\rho}^2$, respectively. The second method, denoted as $M_{\rm b}$ method, uses the stationary bootstrap method described in Sec 4.2 and the resultant systematic error and random error variance will be denoted as $e_{\rm s,b}$ and $e_{\rm r,b}^2$, respectively (see the example given in Fig. 5).

Consistent with the expectation, error estimates from both M_ρ and $M_{\rm b}$ methods are higher for $v_{\rm R,lidar}$ than $v_{\rm r,sonic}$ (Fig. 7) due to the difference in autocorrelation functions. Both methods give very similar estimates of the systematic error, although there

Atmos. Meas. Tech. Discuss., doi:10.5194/amt-2016-83, 2016
Manuscript under review for journal Atmos. Meas. Tech.
Published: 15 March 2016

Atmospheric Measurement Techniques Discussions

are a few cases for which the M_ρ method produces higher systematic errors than the M_b method (Fig. 8). The median of e_s from $v_{\mathrm{R,lidar}}$ is 1.5%/0.9% for T = 30/55 minutes. For the random error, errors from the M_ρ method are always higher than the M_b method due in part to the negative bias in the M_b method (Politis and White, 2004) (Fig. 8). The median of e_r^2 from $v_{\mathrm{R,lidar}}$ is 1.6%/0.9% and 12.7%/9.5% when the error is expressed not as variance but as standard deviation for T = 30/55 minutes, respectively. Despite the expected difference between the errors from the two methods, both methods consistently confirm the trend of decreasing error with increasing sampling duration (Fig. 9), and the relatively close agreement of the results from the two approaches offers empirical support for the relationships between the errors and the autocorrelation function of radial velocity as described by Eqs. (13) and (16) for ergodic and stationary time series.

5 Discussions

On the basis of th empirical evidence presented in Sect. 4, in the following we use the theoretical framework presented in Sec. 3 to describe how the error in estimating radial velocity variance from lidar measurement that results from (i) autocorrelation function, (ii) sampling duration and (iii) sampling interval can be minimized. The first factor (autocorrelation function) is determined by the underlying wind field, the lidar LOS orientation and the size of volumetric averaging (i.e., σ_Q in Eq. (5)). The autocorrelation function needs to be specified to estimate uncertainty in the variance estimates. It typically approximates an exponential but the precise functional form and the rate of decay varies depending on the flow field. Therefore, in practice, error reduction can only be achieved by adjusting the other two factors: sampling duration (T) and sampling interval (δt), with assumption or knowledge of the autocorrelation function $\rho(\tau)$.

Atmospheric turbulence is rarely isotropic, and for all the hours presented in Sect. 4 the three wind components had non-equal variance. However, here we use the isotropic turbulence model to model the autocorrelation function noting that it is always possible to find an integral length scale to reproduce the observed autocorrelation function of radial velocity from lidar measurements with the isotropic turbulence model (Pope, 2000) and the the von Kármán spectra (Burton et al., 2011) (e.g., Fig. 5). Therefore, we argue that with a proper length scale the isotropic turbulence model can generate an autocorrelation function that can be used to approximate non-isotropic turbulence conditions, justifying the use of the isotropic turbulence model here.

Based on the isotropic turbulence model and the von Kármán spectra, the relative systematic error (e_s) is negligible in comparison to the random error. Hence, only the analysis of random error variance (e_r^2) or standard deviation (e_r) is given below. The magnitude of e_r^2 is not sensitive to the sampling interval (δt). Because the integral time scale (τ_0) has the order of magnitude of 10 sec and δt = 1–10 sec, it is likely that $\delta t/\tau_0 < 1$, implying that in practice the sampling interval is a minor factor on error reduction (Fig. 10). Increasing the size of volumetric averaging in terms of σ_Q can cause e_r^2 to increase with a rate that decreases to nearly zero when the sampling duration increases and the LOS moves from being parallel to perpendicular to the wind direction (i.e., β from 0°to 90°) (Fig. 11). Therefore, it is also a minor factor on error reduction when the sampling duration is long. The LOS orientation relative to the wind direction (β) naturally affects the properties of random errors because the time scale of radial velocity varies with β. For example, for the isotropic turbulence model used here, streamwise velocity

Atmos. Meas. Tech. Discuss., doi:10.5194/amt-2016-83, 2016
Manuscript under review for journal Atmos. Meas. Tech.
Published: 15 March 2016

Atmospheric Measurement Techniques Discussions

has the largest time scale and as a result errors are large when the LOS is aligned with the wind direction (i.e., $\beta = 0°$) (Figs. 10a and 11a). In general e_r^2 is not sensitive to β, but it must be acknowledged that the effect of β on e_r^2 will change if a different turbulence model is applied. The factor that has the most significant effect on error reduction is the sampling duration (Figs. 10 and 11). Thus optimization of lidar operation for retrieval of radial velocity variance can be considered through the lens of "how long is long enough?" (Lenschow et al., 1994). Provided that the optimum six beam configuration proposed in Sathe et al. (2015) (i.e., $\phi = 45°$) is applied to the Galion lidar for which $\sigma_Q = 15.4\,\mathrm{m}$ under neutral atmospheric conditions over flat terrain, both the systematic and random errors are almost independent of LOS orientation and surface roughness length which is used to predict the integral length scale and turbulence intensity (Fig. 12). The systematic error is lower than 1.0% when $T > 30$ minutes (Fig. 12). The standard deviation (e_r) of random errors can be reduced from 12.0% to 9.0% by increasing the sampling duration from 30 minutes to 60 minutes (Fig. 12), which is consistent with the observed 12.7%–9.5% in Sec. 4.3. The standard deviation remains higher than 6.0% when T increases to 120 minutes (Fig. 12). Note that the volumetric averaging increases e_r by less than 1.0% because of its relatively small size ($\sigma_Q/L_1 < 0.1$). The implication of the analysis above is that, given that 0.5–1.0 hour is usually the length over which the stationarity assumption is valid in the ABL (Larsén et al., 2016) the random error in radial velocity variance estimates will likely be around 10.0% and it will be difficult to estimate radial velocity variance with random errors lower than 5.0%.

6 Concluding remarks

Use of lidar for estimation of turbulence fields if realized could revolutionize atmospheric boundary layer characterization studies and has applications to many fields. Accurate radial velocity variance estimates are necessary (but not sufficient) to obtaining robust turbulence statistics from lidar. The accuracy of radial velocity variance estimates and their relationship to pseudo-point measurements from sonic anemometers are determined by (i) the applicability of the stationarity assumption, (ii) the effect of volumetric averaging on the radial velocity autocorrelation function, (iii) the sampling interval, and (iv) the sampling duration. Of these factors (i) the stationarity assumption is determined only by atmospheric conditions but is most likely to be achieved within the period of one hour in environments where the surface conditions are homogeneous. The second factor (ii) the volumetric averaging is dictated by the probe length that is determined by the lidar properties; it causes the radial velocity autocorrelation function to increase and thus increases errors in radial velocity variance estimates. Large probe length can result in high errors. The third factor (iii) the sampling interval is determined partly by the scan geometry which is needed to sample radial velocities with different LOS orientations to reconstruct the wind field, and partly by the lidar configurations of e.g. the dwell time of each measurement and the scanning speed. Errors are not sensitive to the sampling interval because the sampling interval for lidar turbulence measurement is commonly smaller than the turbulence integral time scale. The last factor (iv) the sampling duration, which together with the sampling interval determines the number of samples available for radial velocity estimates, can only be extended to the limit implied by the stationarity assumption, but in principle as sampling duration icreases the errors associated with the radial velocity variance decreases.

Atmos. Meas. Tech. Discuss., doi:10.5194/amt-2016-83, 2016
Manuscript under review for journal Atmos. Meas. Tech.
Published: 15 March 2016

Atmospheric Measurement Techniques Discussions

Given these constraints on radial velocity variance estimates, this paper uses theories and empirical observations to show that for sample periods for which stationarity can reasonably be asserted (approximately one hour), the systematic error can be reduced to a level lower than 1% and the standard deviation of random errors will be around 10%. These errors will propagate through to estimation of turbulence statistics from lidar measurements and thus provide a fundamental limit on the likely accuracy of those estimates.

Acknowledgements. This work was funded by the US National Science Foundation (Award No. 1464383 and 1540393) and the US Department of Energy (Award No. DE-EE0005379).

Atmos. Meas. Tech. Discuss., doi:10.5194/amt-2016-83, 2016
Manuscript under review for journal Atmos. Meas. Tech.
Published: 15 March 2016

References

Banta, R. M., Pichugina, Y. L., Kelley, N. D., Hardesty, R. M., and Brewer, W. A.: Wind energy meteorology: Insight into wind properties in the turbine-rotor layer of the atmosphere from high-resolution Doppler lidar, B. Am. Meteorol. Soc., 94, 883–902, doi:10.1175/BAMS-D-11-00057.1, 2013.

Barthelmie, R. J., Wang, H., Doubrawa, P., Giroux, G., and Pryor, S. C.: Effects of an escarpment on flow parameters of relevance to wind turbines, Wind Energy, doi:10.1002/we.1980, 2016.

Box, G. E. P., Jenkins, G. M., Reinsel, G. C., and Ljung, G. M.: Time Series Analysis: Forecasting and Control, John Wiley & Sons, 2015.

Branlard, E., Pedersen, A. T., Mann, J., Angelou, N., Fischer, A., Mikkelsen, T., Harris, M., Slinger, C., and Montes, B. F.: Retrieving wind statistics from average spectrum of continuous-wave lidar, Atmos. Meas. Tech., 6, 1673–1683, doi:10.5194/amt-6-1673-2013, 2013.

Burton, T., Sharpe, D., Jenkins, N., and Bossanyi, E.: Wind energy handbook, John Wiley & Sons, 2011.

Clifton, A., Elliott, D., and Courtney, M.: Ground-based vertically profiling remote sensing for wind resource assessment, report, IEA Wind, available at: https://www.ieawind.org/index_page_postings/RP/RP%2015_RemoteSensing_1stEd_8March2013.pdf, (last access: 28 February 2016), 2013.

Foken, T. and Wichura, B.: Tools for quality assessment of surface-based flux measurements, Agric. For. Meteorol., 78, 83–105, doi:10.1016/0168-1923(95)02248-1, 1996.

Gottschall, J., Courtney, M. S., Wagner, R., Jørgensen, H. E., and Antoniou, I.: Lidar profilers in the context of wind energy–A verification procedure for traceable measurements, Wind Energy, 15, 147–159, doi:10.1002/we.518, 2012.

Kristensen, L., Kirkegaard, P., and Mikkelsen, T.: Determining the velocity fine structure by a laser anemometer with fixed orientation, Tech. Rep. Risø-R-1762(EN), Technical University of Denmark, available at: http://orbit.dtu.dk/fedora/objects/orbit:86624/datastreams/file_5712483/content, (last access: 28 February 2016), 2011.

Larsén, X. G., Larsen, S. E., and Petersen, E. L.: Full-scale spectrum of boundary-layer winds, Bound.-Layer Meteor., pp. 1–23, doi:10.1007/s10546-016-0129-x, 2016.

Lenschow, D. H., Mann, J., and Kristensen, L.: How long is long enough when measuring fluxes and other turbulence statistics?, J. Atmos. Oceanic Technol., 11, 661–673, doi:10.1175/1520-0426(1994)011<0661:HLILEW>2.0.CO;2, 1994.

Lindelöw-Marsden, P.: UpWind D1. Uncertainties in wind assessment with LIDAR, Tech. Rep. Risø-R-1681(EN), Technical University of Denmark, available at: http://orbit.dtu.dk/fedora/objects/orbit:82842/datastreams/file_5113517/content (last access: 28 February 2016), 2009.

Mann, J., Cariou, J.-P., Courtney, M. S., Parmentier, R., Mikkelsen, T., Wagner, R., Lindelöw, P., Sjöholm, M., and Enevoldsen, K.: Comparison of 3D turbulence measurements using three staring wind lidars and a sonic anemometer, IOP Conf. Ser.: Earth Environ. Sci., 1, 012 012, doi:10.1088/1755-1315/1/1/012012, 2008.

Mann, J., Peña, A., Bingöl, F., Wagner, R., and Courtney, M. S.: Lidar scanning of momentum flux in and above the atmospheric surface layer, J. Atmos. Oceanic Technol., 27, 959–976, doi:10.1175/2010JTECHA1389.1, 2010.

Newman, J. F., Klein, P. M., Wharton, S., Sathe, A., Bonin, T. A., Chilson, P. B., and Muschinski, A.: Evaluation of three lidar scanning strategies for turbulence measurements, Atmos. Meas. Tech. Discuss., 8, 12 329–12 381, doi:10.5194/amtd-8-12329-2015, 2015.

Politis, D. N. and Romano, J. P.: The stationary bootstrap, J. Amer. Statist. Assoc., 89, 1303–1313, doi:10.1080/01621459.1994.10476870, 1994.

Politis, D. N. and White, H.: Automatic block-length selection for the dependent bootstrap, Econom. Rev., 23, 53–70, doi:10.1081/ETC-120028836, 2004.

Pope, S. B.: Turbulent flows, Cambridge University Press, 2000.

Sathe, A. and Mann, J.: Measurement of turbulence spectra using scanning pulsed wind lidars, J. Geophys. Res., 117, D01 201, doi:10.1029/2011JD016786, 2012.

Sathe, A. and Mann, J.: A review of turbulence measurements using ground-based wind lidars, Atmos. Meas. Tech., 6, 3147–3167, doi:10.5194/amt-6-3147-2013, 2013.

Sathe, A., Mann, J., Vasiljevic, N., and Lea, G.: A Six-Beam Method to Measure Turbulence Statistics Using Ground-Based Wind Lidars, Atmos. Meas. Tech., 8, 729–740, doi:10.5194/amt-8-729-2015, 2015.

Taylor, G. I.: The spectrum of turbulence, Proc. Roy. Soc. London, 164, 476–490, doi:10.1098/rspa.1938.0032, 1938.

TurbSim: TurbSim, available at: https://nwtc.nrel.gov/TurbSim, (last access: 28 February 2016), 2016.

Wang, H., Barthelmie, R. J., Pryor, S. C., and Brown, G.: Lidar arc scan uncertainty reduction through scanning geometry optimization, Atmos. Meas. Tech. Discuss., 8, 10 429–10 471, doi:10.5194/amtd-8-10429-2015, 2015.

Atmos. Meas. Tech. Discuss., doi:10.5194/amt-2016-83, 2016
Manuscript under review for journal Atmos. Meas. Tech.
Published: 15 March 2016

Atmospheric Measurement Techniques Discussions

Table A1. Nomenclature.

β	Angle between the wind direction and lidar laser beam [°]
δt	Lidar radial velocity samping interval [sec]
θ	Lidar azimuth angle [°]
μ_1	Ensemble mean of a random variable
$\mu_1(T)$	Estimated mean of a random variable over a mpling duration T
$\mu_{1,\mathrm{r}}(T)$	Estimated mean of the point radial velocity over a sampling duration T [$\mathrm{m\,s^{-1}}$]
μ_2	Ensemble variance of random variable
$\mu_2(T)$	Estimated variance of a random variable over a mpling duration T
$\mu_{2,\mathrm{R}}$	Ensemble variance of the averaged radial velocity [$\mathrm{m^2\,s^{-2}}$]
$\mu_{2,\mathrm{r}}$	Ensemble variance of the point radial velocity [$\mathrm{m^2\,s^{-2}}$]
$\mu_{2,\mathrm{r}}(T)$	Estimated variance of the point radial velocity over a sampling duration T [$\mathrm{m^2\,s^{-2}}$]
ρ_{R}	Autocorrelation of the averaged radial velocity
ρ_{r}	Autocorrelation of the point radial velocity
σ_{Q}	Standard deviation of radial velocity weight function [m]
τ	Autocorrelation time lag [sec]
τ_0	Integral time scale [sec]
ϕ	Lidar elevation angle [°]
D_{r}	Structure function [$\mathrm{m^2\,s^{-2}}$]
$E^2_{\mathrm{r,r}}$	Random error variance in variance estimates using point radial velocities [$\mathrm{m^4\,s^{-4}}$]
$E_{\mathrm{r,s}}$	Systematic error in variance estimates using point radial velocities [$\mathrm{m^2\,s^{-2}}$]
$\boldsymbol{e}_1$	Unit vector in streamwise direction [m]
e^2_{r}	Relative variacne of random errors
$e^2_{\mathrm{r},\rho}$	Relative variance of random errors estimated using autocorrelation function
$e^2_{\mathrm{r,b}}$	Relative variance of random errors estimated using the bootstrap method
$e^2_{\mathrm{r,R}}$	Relative variance of random errors in variance estimates using averaged radial velocities
$e^2_{\mathrm{r,r}}$	Relative variance of random errors in variance estimates using point radial velocities
e_{s}	Relative systematic error
$e_{\mathrm{s},\rho}$	Relative systematic error estimated using autocorrelation function
$e_{\mathrm{s,b}}$	Relative systematic error estimated using the bootstrap method
$e_{\mathrm{s,R}}$	Relative systematic error in variance estimates using averaged radial velocities
$e_{\mathrm{s,r}}$	Relative systematic error in variance estimates using point radial velocities
L_1	Integral length scale of the streamwise velocity [m]

Atmos. Meas. Tech. Discuss., doi:10.5194/amt-2016-83, 2016
Manuscript under review for journal Atmos. Meas. Tech.
Published: 15 March 2016

Atmospheric Measurement Techniques Discussions

Table A1. Continued.

L_{R}	Integral length scale of the averaged radial velocity [m]
L_{r}	Integral length scale of the point radial velocity [m]
N	Radial velocity sample number
N_{b}	Repetition time of bootstrap sampling
N_{T}	Sampling numbers obtained during sampling duration T
N_{n}	Sampling numbers obtained during sampling duration T_{n}
$\boldsymbol{n}$	Unit directional vector of lidar line of sight
Q	Radial velocity weighting function
R_{ij}	Wind velocity covariance tensor [$\mathrm{m^2\,s^{-2}}$]
R_{R}	Covariance of the averaged radial velocity [$\mathrm{m^2\,s^{-2}}$]
R_{r}	Covariance of the point radial velocity [$\mathrm{m^2\,s^{-2}}$]
r_1	Spatial lag in the streamwise direction [m]
s	Lidar range gate location [m]
s'	Lidar range distance [m]
s''	Lidar range distance [m]
T	Sampling duration of a full time series [sec]
T_{n}	Sampling duration of a subset of time series [sec]
t	Measurement time stamp [sec]
U_1	Mean streamwise velocity [$\mathrm{m\,s^{-1}}$]
$\boldsymbol{u}$	Wind velocity vector [$\mathrm{m\,s^{-1}}$]
u_1	Streamwise velocity component [$\mathrm{m\,s^{-1}}$]
u_2	Transverse velocity component [$\mathrm{m\,s^{-1}}$]
u_3	Vertical velocity component [$\mathrm{m\,s^{-1}}$]
v_{R}	Averaged radial velocity [$\mathrm{m\,s^{-1}}$]
$v_{\mathrm{R,lidar}}$	Radial velocity measured by lidars [$\mathrm{m\,s^{-1}}$]
v_{r}	Point radial velocity [$\mathrm{m\,s^{-1}}$]
$v_{\mathrm{r,sonic}}$	Radial velocity measured by sonic anemometers [$\mathrm{m\,s^{-1}}$]
$\boldsymbol{x}$	Position vector vector [m]
x_1	Coordinate in the streamwise direction [m]
x_2	Coordinate in the transverse direction [m]
x_3	Coordinate in the vertical direction [m]
z_0	Surface roughness length [m]

Atmos. Meas. Tech. Discuss., doi:10.5194/amt-2016-83, 2016
Manuscript under review for journal Atmos. Meas. Tech.
Published: 15 March 2016

Atmospheric Measurement Techniques Discussions

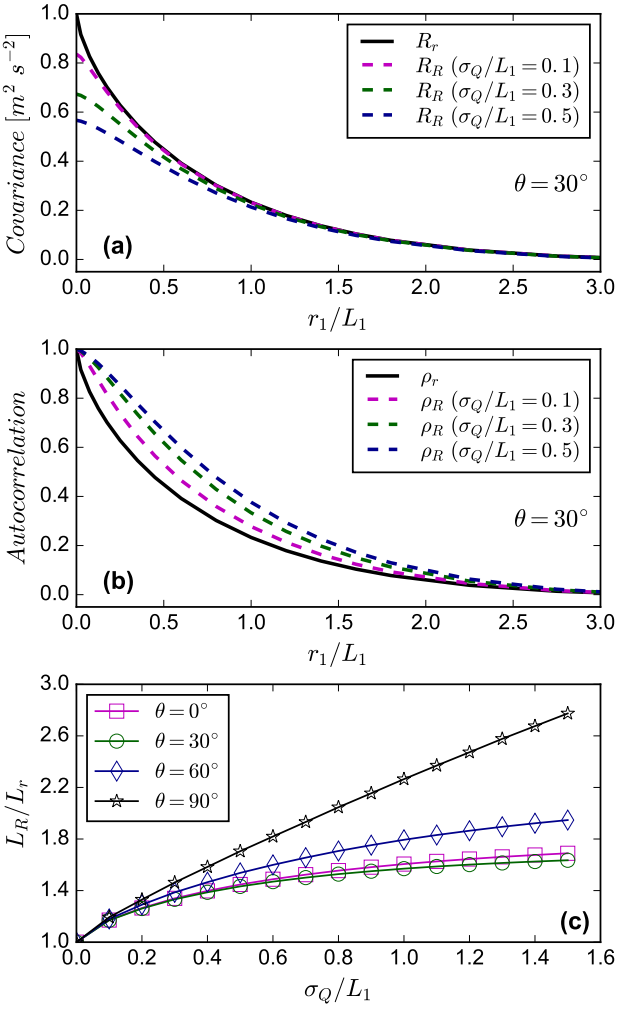

Figure 1. Examples of turbulence statistics of point radial velocity (v_r) and averaged radial velocity (v_R) derived from Eqs. (6) and (7) using the isotropic turbulence model (Pope, 2000) and the von Kármán spectra (Burton et al., 2011) with streamwise velocity U_1 = 8 m s^{-1}, turbulence intensity = 12.5 %, and lidar elevation angle = 10°. The covariance and autocorrelation functions for v_r (R_r and ρ_r) and v_R (R_R and ρ_R) for azimuth angle θ = 30° are shown in (**a**) and **b**, respectively, as functions of r_1/L_1 where r_1 is the spatial lag in streamwise direction and L_1 is the integral length scale of streamwise velocity. R_R and ρ_R are presented in terms of σ_Q/L_1 where σ_Q represents the size of volumetric averaging (see Eq. (5)). The effect of volumetric averaging on the integral length scale of radial velocity is presented in (**c**) in terms of the relationship between $L_\mathrm{R}/L_\mathrm{r}$ and σ_Q/L_1 for different θ values where L_r and L_R are the integral length scales for v_r and v_R, respectively.

Atmos. Meas. Tech. Discuss., doi:10.5194/amt-2016-83, 2016
Manuscript under review for journal Atmos. Meas. Tech.
Published: 15 March 2016

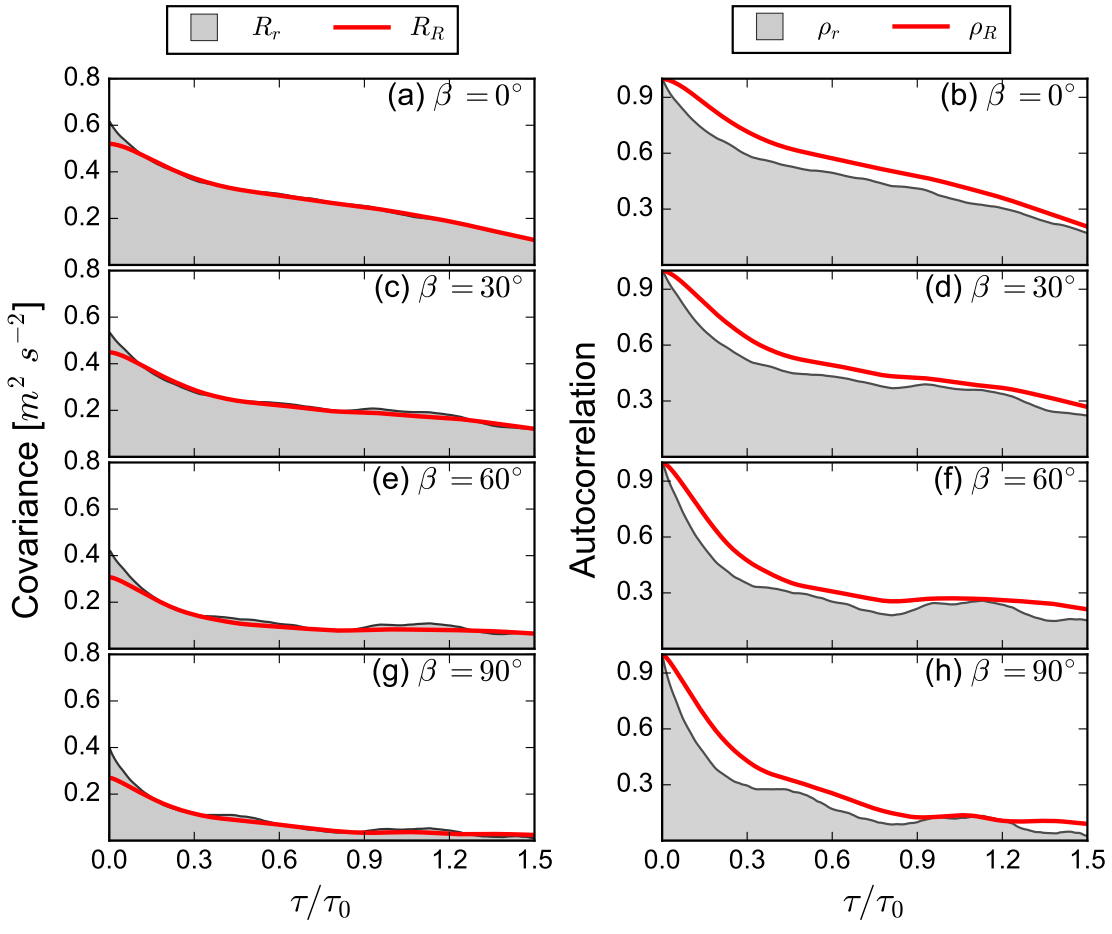

Figure 2. Covariance (R_r and R_r on the left) and autocorrelation functions (ρ_r and ρ_r on the right) of the point radial velocity (v_r) and averaged radial velocity (v_R) derived from statistically simulated time series using TurbSim (2016) with the SMOOTH model and the default parameter values. Covariance and autocorrelation functions are presented for four different LOS orientations here as indicated by the angle of LOS relative to the mean wind direction (β). The time lag (τ) is normalized by τ_0 which is the first time when $\rho_r = 1/e$ at $\beta = 0$. A fixed elevation angle of 10° is used.

Atmos. Meas. Tech. Discuss., doi:10.5194/amt-2016-83, 2016
Manuscript under review for journal Atmos. Meas. Tech.
Published: 15 March 2016

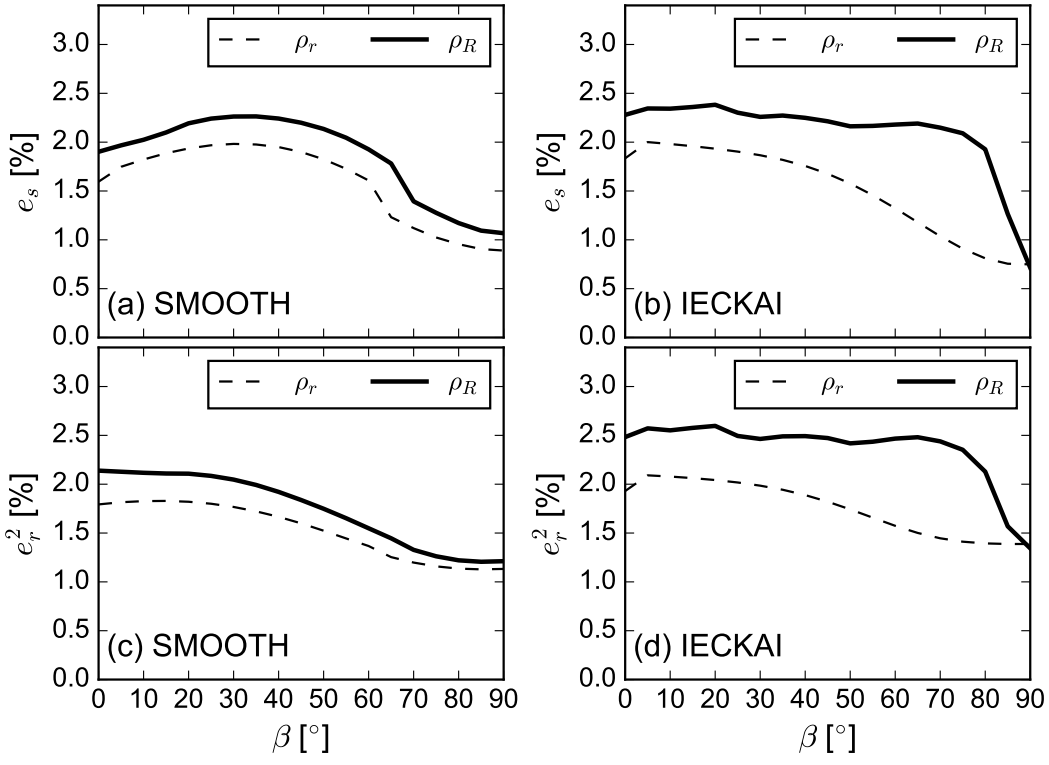

Figure 3. The relative systematic error (e_s) and random error variance (e_r^2) derived from the autocorrelation functions of the simulated point radial velocity (ρ_r) and averaged radial velocity (ρ_R) from the SMOOTH model in (**a**) and (**c**) and from the IECKAI model in (**b**) and (**d**) (TurbSim, 2016) as functions of the angle between the LOS and mean wind direction (β). The sampling duration is $100\tau_0$ where τ_0 is the first time when the point radial velocity autocorrelation crosses $1/e$ at $\beta = 0°$.

Atmos. Meas. Tech. Discuss., doi:10.5194/amt-2016-83, 2016
Manuscript under review for journal Atmos. Meas. Tech.
Published: 15 March 2016

Atmospheric Measurement Techniques Discussions

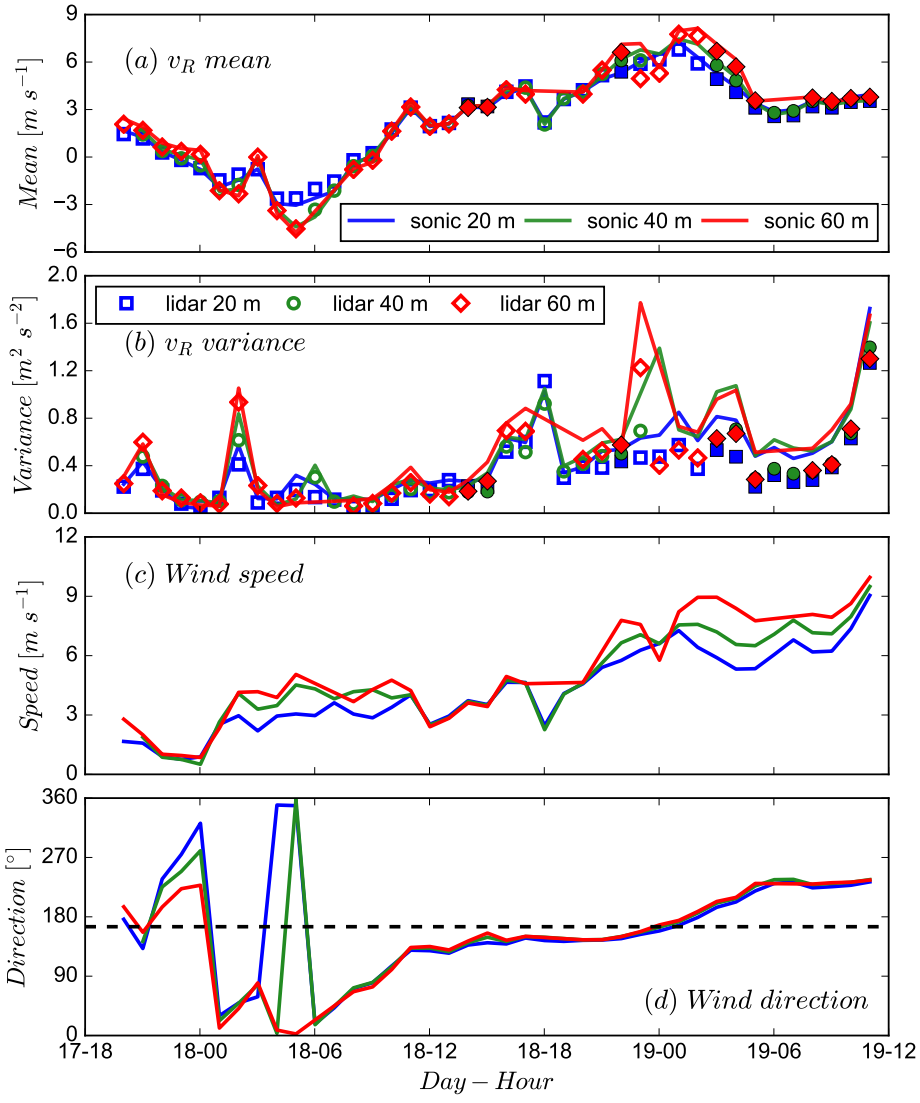

Figure 4. Time series of (**a**) hourly mean and (**b**) variance of radial velocity (v_R) from the lidar (markers) and the sonic anemometers (lines) and time series of (**c**) hourly mean wind speed and (**d**) direction from the sonic anemometers at three different heights. The mean and variance of radial velocity from the hourly time series classified as stationary using the method of Foken and Wichura (1996) are shown by the filled markers. The dash line in (**d**) gives the wind direction under which the sonic anemometers are in the center of the wind turbine wake.

Atmos. Meas. Tech. Discuss., doi:10.5194/amt-2016-83, 2016
Manuscript under review for journal Atmos. Meas. Tech.
Published: 15 March 2016

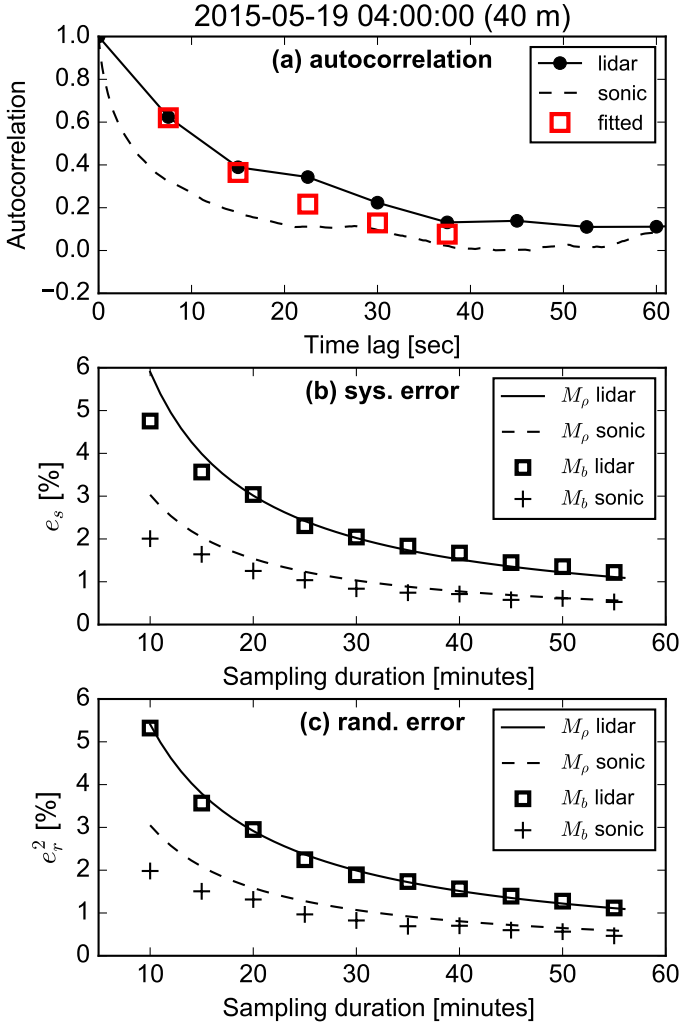

Figure 5. An example of the autocorrelation and errors in radial velocity variance estimate using data from the hour starting at 2015-05-19 04:00 at 40 m height. The autocorrelation functions derived from the lidar and sonic measurements are presented in (**a**). Systematic errors (e_s) and random errors (e_r^2) are presented in (**b**) and (**c**), respectively. Errors associated with both lidar and sonic anemometer data are estimated using the autocorrelation function from measurements (denoted by M_ρ) and the stationary bootstrap method (denote by M_b) described in Sect. 4.2.

Atmos. Meas. Tech. Discuss., doi:10.5194/amt-2016-83, 2016
Manuscript under review for journal Atmos. Meas. Tech.
Published: 15 March 2016

Atmospheric Measurement Techniques Discussions

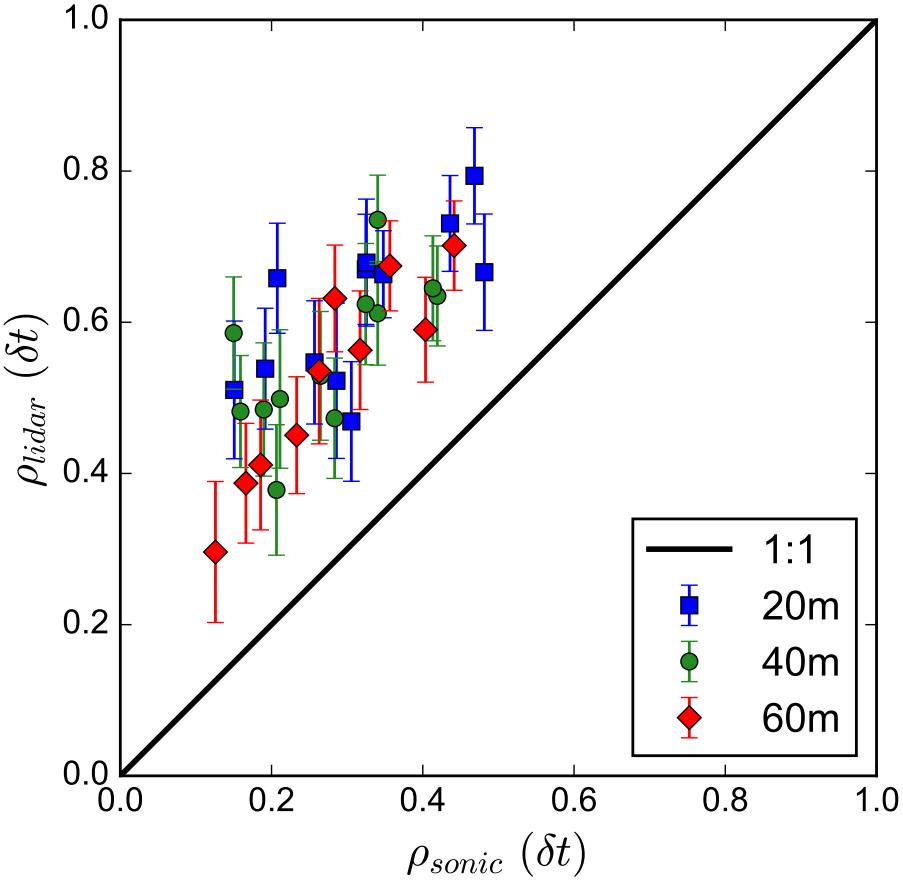

Figure 6. Comparison of the values of radial velocity autocorrelation function from the sonic data (ρ_{sonic}) and the lidar data (ρ_{lidar}) at the first time lag δt = 7.5 sec. The 95% confidence interval of ρ_{lidar} is indicated by the error bar.

Atmos. Meas. Tech. Discuss., doi:10.5194/amt-2016-83, 2016
Manuscript under review for journal Atmos. Meas. Tech.
Published: 15 March 2016

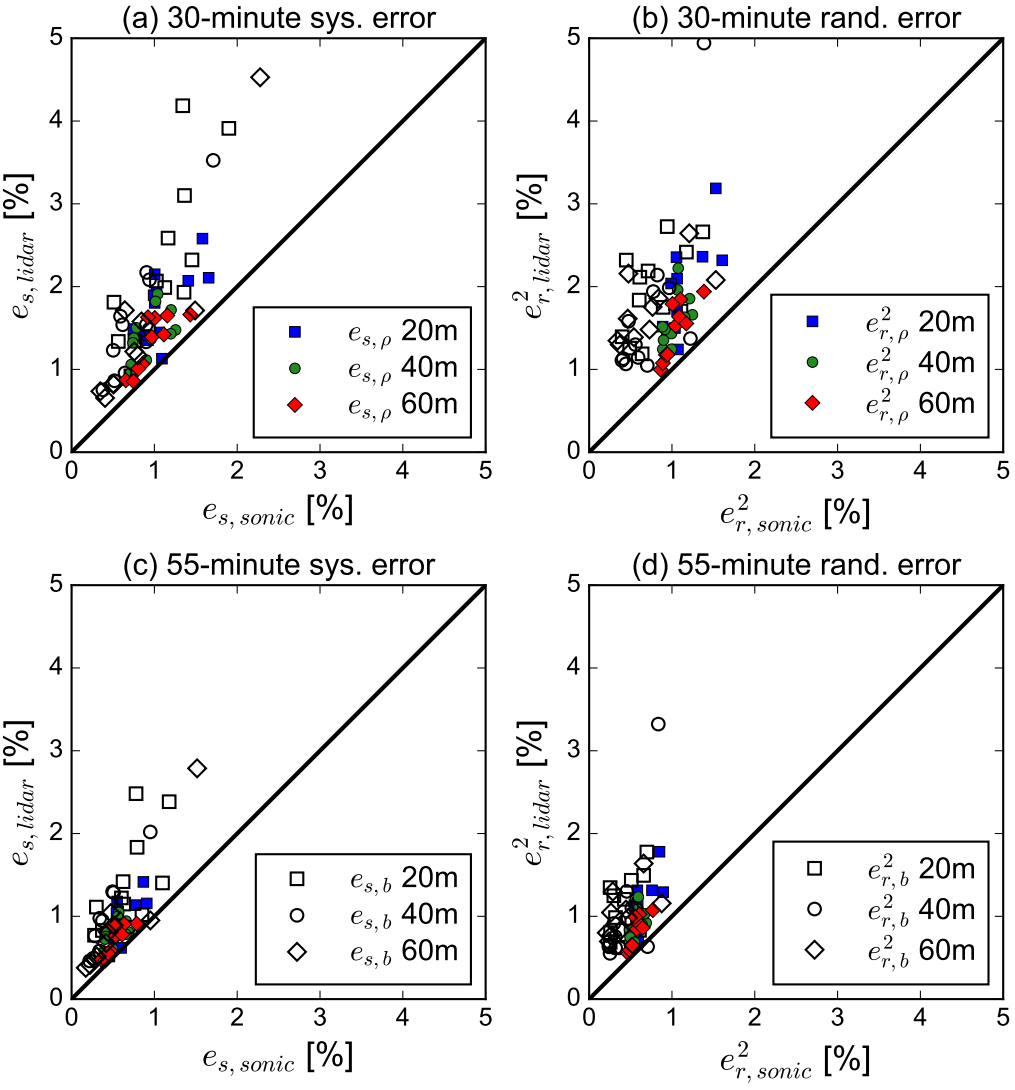

Figure 7. Comparison of the systematic error estimated from the sonic data ($e_{\mathrm{s,sonic}}$) and from the lidar data ($e_{\mathrm{s,lidar}}$) in (**a**) for a sampling duration of 30 minutes and (**c**) a sampling duration of 55 minutes, and comparison of the random error estimated from the sonic data ($e^2_{\mathrm{r,sonic}}$) and from the lidar data ($e^2_{\mathrm{r,lidar}}$) in (**b**) for a sampling duration of 30 minutes and (**d**) a sampling duration of 55 minutes. The method used to estimate the errors is indicated by the subscript in the legend where ρ denotes the M_ρ method using the autocorrelation function and b denotes the M_b method using the stationary bootstrap method. The solid lines are the 1:1 lines.

Atmos. Meas. Tech. Discuss., doi:10.5194/amt-2016-83, 2016
Manuscript under review for journal Atmos. Meas. Tech.
Published: 15 March 2016

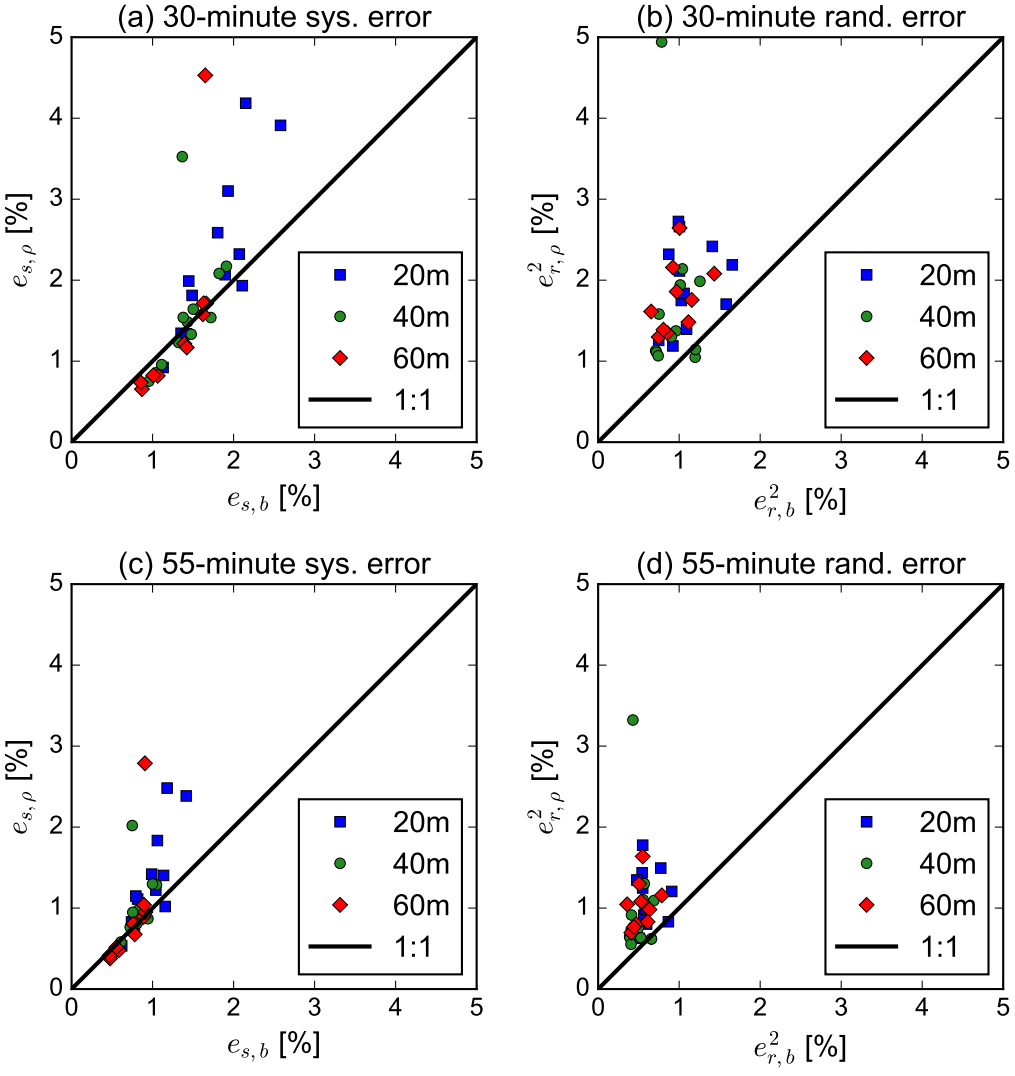

Figure 8. Comparison of the lidar radial velocity systematic errors $e_{\mathrm{s},\rho}$ and $e_{\mathrm{s,b}}$ estimated using the autocorrelation (M_ρ) method and the stationary bootstrap (M_b) method, respectively, for (**a**) a sampling duration of 30 minutes and (**c**) a sampling duration of 55 minutes, and comparison of the lidar radial velocity random errors $e^2_{\mathrm{r},\rho}$ and $e^2_{\mathrm{r,b}}$ estimated using the M_ρ method and the M_b method, respectively, for (**b**) a sampling duration of 30 minutes and (**d**) a sampling duration of 55 minutes. The measurement heights can be found in the legend.

Atmos. Meas. Tech. Discuss., doi:10.5194/amt-2016-83, 2016
Manuscript under review for journal Atmos. Meas. Tech.
Published: 15 March 2016

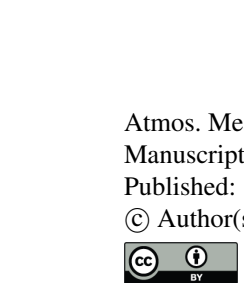

Atmospheric Measurement Techniques Discussions

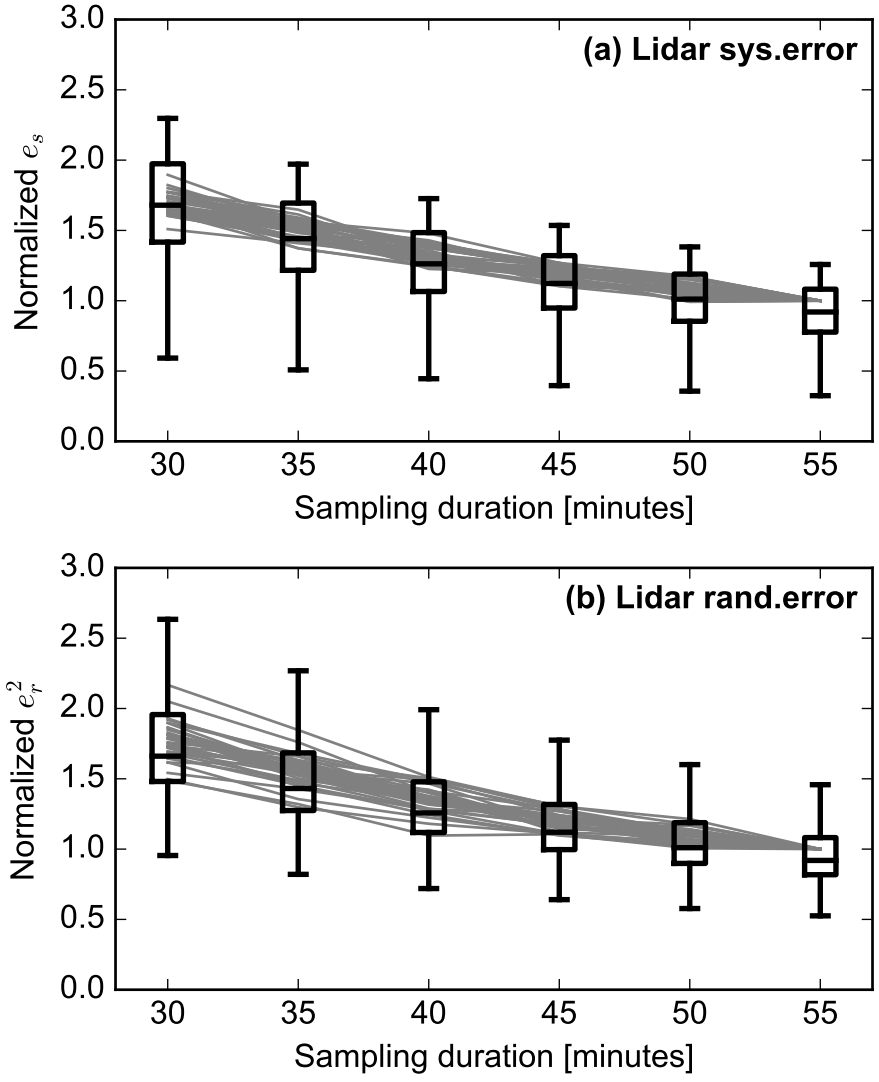

Figure 9. Relationships between (**a**) the systematic error (e_s) and the sampling duration and (**b**) the random error (e_r^2) and the sampling duration for radial velocity variance estimated from the lidar data using the autocorrelation method (gray lines) and the stationary bootstrap method (boxplots). The errors are normalized by the respective errors estimated from the autocorrelation method with the sampling duration of 55 minutes.

Atmos. Meas. Tech. Discuss., doi:10.5194/amt-2016-83, 2016
Manuscript under review for journal Atmos. Meas. Tech.
Published: 15 March 2016

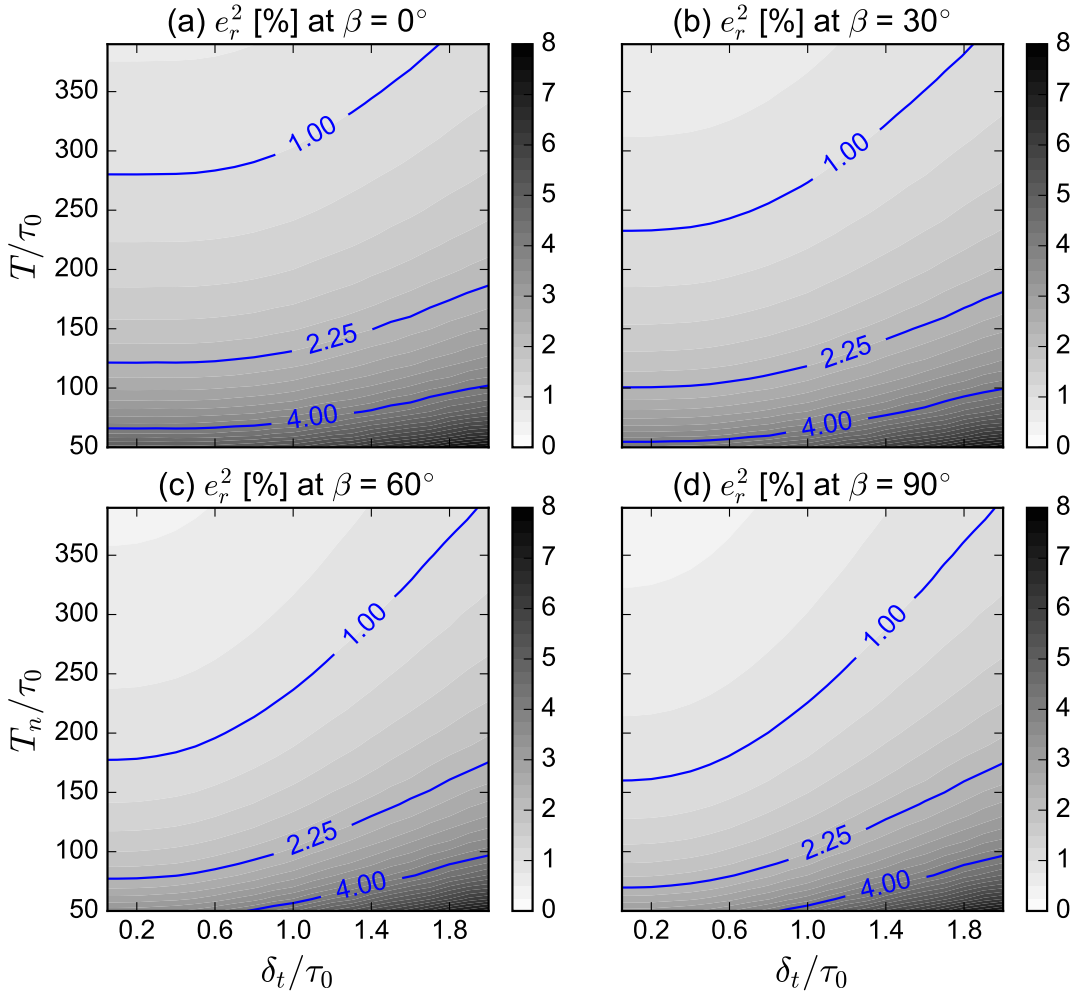

Figure 10. Contours of the relative variance (e_r^2) of random errors of radial velocity variance from lidar measurements estimated with the isotropic turbulence model (Pope, 2000) and the von Kármán spectra (Burton et al., 2011) as a function of the sampling duration (T) and the sampling interval (δt) normalized by the integral time scale (τ_0) for four different β values where β is the angle between the LOS and the wind direction. The weighting function (Eq. (5)) representing the volumetric averaging has a standard deviation $\sigma_Q = 0.2L_1$ where L_1 is the streamwise integral length scale. The other input parameters include the elevation angle $\phi = 10°$ and the mean wind speed $U_1 = 8\,\mathrm{m\,s^{-1}}$.

Atmos. Meas. Tech. Discuss., doi:10.5194/amt-2016-83, 2016
Manuscript under review for journal Atmos. Meas. Tech.
Published: 15 March 2016

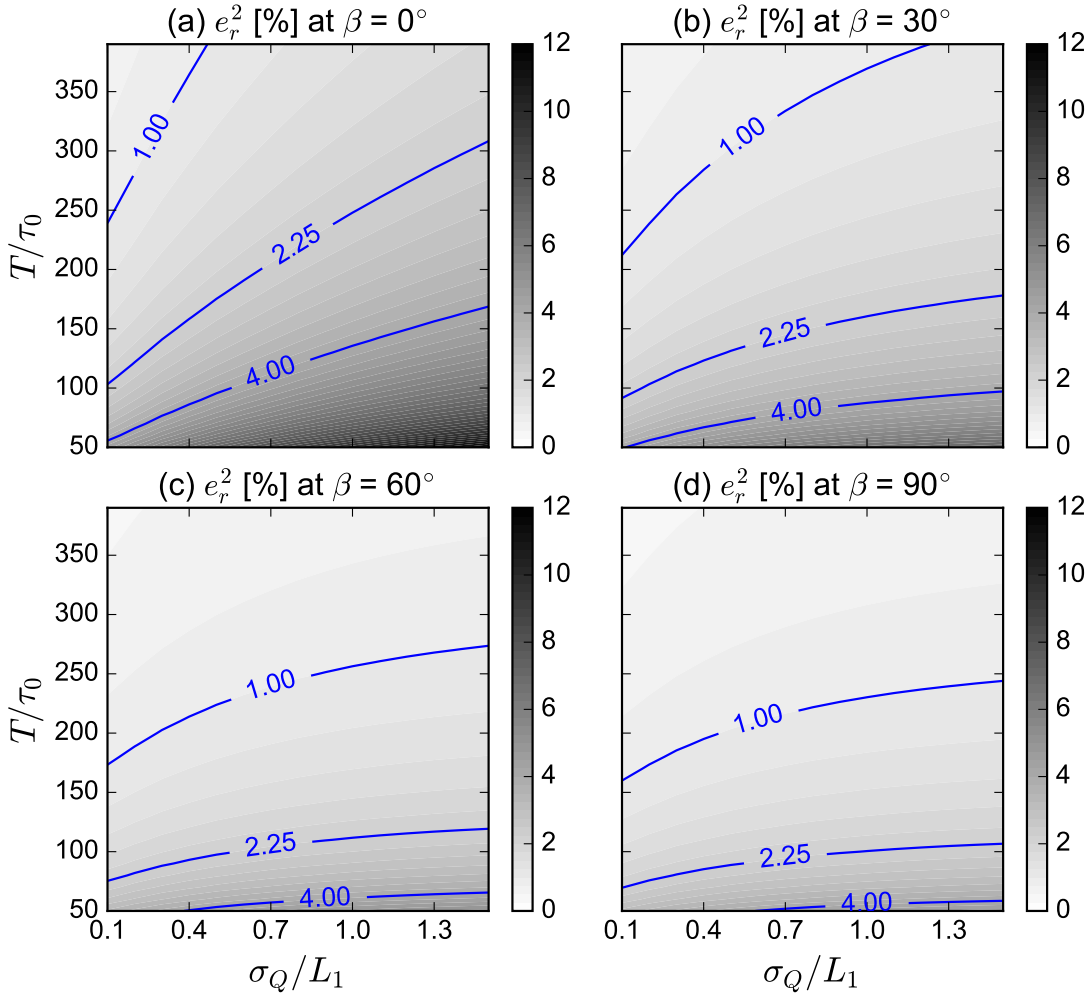

Figure 11. Contours of the relative variance (e_r^2) of random errors of radial velocity variance from lidar measurements estimated with the isotropic turbulence model (Pope, 2000) and the von Kármán spectra (Burton et al., 2011) as a function of the sampling duration (T) normalized by the integral time scale (τ_0) and the volumetric averaging size (σ_Q) normalized by the streamwise integral length scale (L_1) for four different β values where β is the angle between the LOS and the wind direction. The other input parameters include the sampling interval $\delta t = 0.5\tau_0$, the elevation angle $\phi = 10°$ and the mean wind speed $U_1 = 8\,\mathrm{m\,s^{-1}}$.

Atmos. Meas. Tech. Discuss., doi:10.5194/amt-2016-83, 2016
Manuscript under review for journal Atmos. Meas. Tech.
Published: 15 March 2016

Atmospheric Measurement Techniques Discussions

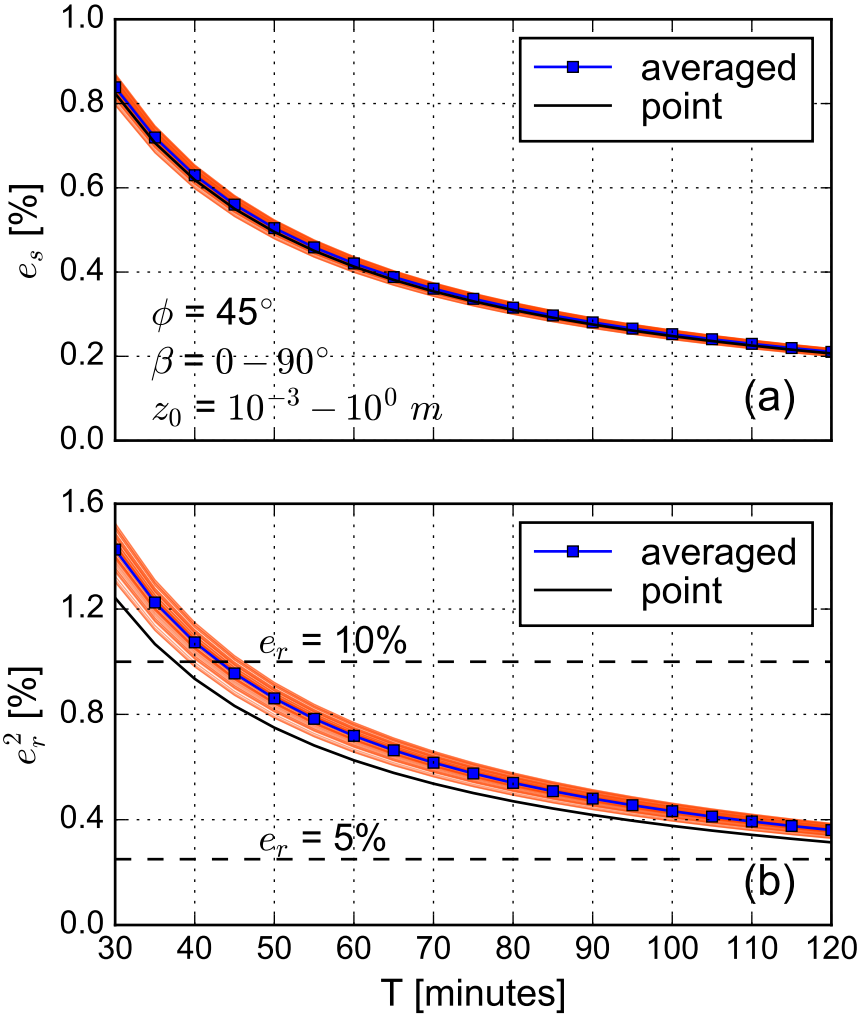

Figure 12. Variation of the systematic error (e_s) and variance of random error (e_r^2) with respect to the sampling duration (T) in (**a**) and (**b**), respectively, predicted from the isotropic turbulence model (Pope, 2000) and the von Kármán spectra (Burton et al., 2011) at 80 m height under neutral conditions for surface roughness lengths (z_0) from 10^{-3} m to 10^{0} m and LOS orientations β from 0° to 90° where β is the angle between the LOS and the wind direction. The blue lines with squares and the dark lines are the mean error values from the entire range of z_0 and β for the averaged and point radial velocity variance, respectively. The red shaded areas denote the range of errors of the averaged radial variance. The equation used to estimate the integral length scale can be found in Wang et al. (2015) with a mean wind speed of 7 m s^{-1} and the Coriolis parameter of 10^{-4} s^{-1}. The elevation angle $\phi = 45°$.